

Interaction Event Forecasting in Multi-Relational Recursive HyperGraphs: A Temporal Point Process Approach

Tony Gracious
Ambedkar Dukkipati
tonygracious@iisc.ac.in
ambedkar@iisc.ac.in

Department of Computer Science and Automation,
Indian Institute of Science Bangalore
India

ABSTRACT

Modeling the dynamics of interacting entities using an evolving graph is an essential problem in fields such as financial networks and e-commerce. Traditional approaches focus primarily on pairwise interactions, limiting their ability to capture the complexity of real-world interactions involving multiple entities and their intricate relationship structures. This work addresses the problem of forecasting higher-order interaction events in multi-relational recursive hypergraphs. This is done using a dynamic graph representation learning framework that can capture complex relationships involving multiple entities. The proposed model, *Relational Recursive Hyperedge Temporal Point Process* (RRHyperTPP) uses an encoder that learns a dynamic node representation based on the historical interaction patterns and then a hyperedge link prediction based decoder to model the event's occurrence. These learned representations are then used for downstream tasks involving forecasting the type and time of interactions. The main challenge in learning from hyperedge events is that the number of possible hyperedges grows exponentially with the number of nodes in the network. This will make the computation of negative log-likelihood of the temporal point process expensive, as the calculation of survival function requires a summation over all possible hyperedges. In our work, we use noise contrastive estimation to learn the parameters of our model, and we have experimentally shown that our models perform better than previous state-of-the-art methods for interaction forecasting.

CCS CONCEPTS

• **Computing methodologies** → **Unsupervised learning; Learning latent representations; Knowledge representation and reasoning; Temporal reasoning.**

KEYWORDS

Temporal Networks, Graph Neural Networks, Representation Learning, Hypergraphs, Temporal Point Processes

1 INTRODUCTION

With the rise in the field of geometric deep learning, there is a new interest in learning representations from higher-order relations in networks [3, 4]. These works mostly focused on hypergraphs where relations are represented as hyperedges that represent interactions of groups of entities/nodes [1, 14, 22]. With the availability of richer

datasets and better computational facilities one can go beyond hypergraphs by incorporating a wide variety of information associated with the interaction. These ideas are being explored in recent works of topology-aware deep learning where higher-order network structures such as simplicial complexes, cell complexes, and multi-scale topological information are used for improving graph neural networks [16, 18]. Recent works have shown that n-ary facts or multi-relational hyperedges are the natural data representations for Knowledge graphs, and models based on those perform better than that use pairwise multi-relation models [12, 32].

Most of these works ignore the temporal aspects of the network, where entities interact and evolve. This has been addressed using dynamic network models based on temporal point processes (TPP) and link prediction. The existing works model interactions as instantaneous edges [5, 10, 21, 30]/hyperedges [15] forming between a pair of nodes or a group of nodes, and a generative model is parameterized to model the formation of edges given the history. However, real-world interactions can be much more complex than just a group of entities interacting. These interactions can exhibit group structure within themselves. For example, a directed hyperedge involves interaction between two groups of entities in the source and destination. Here, one can represent the source and destination as hyperedges which act as nodes to the interaction hyperedge. In our work, we generalize this recursive group structure property of real-world interactions to incorporate a variable number of groupings. Examples of these types of interaction can be seen in email exchanges, where there are sender, recipients, and carbon-copied recipients (CCed) addresses. Each group except the sender can have a variable number of addresses, and CCed group is not always present in an email exchange. Similarly, in citation networks, the authors of a scientific article are ordered according to their contributions to the work. Here, the author's position is the grouping, and multiple authors can be in the same position.

We use a multi-relational recursive hyperedges structure to incorporate these complex higher-order interactions. Here, hyperedges can act as nodes in other hyperedges (like CCed or receiver groups in email interactions) and contain relation types indicating their role in the interactions. Then a TPP is defined with these hyperedges as event types with conditional intensity function parameterized using representations/embeddings of the nodes and relations involved in the interactions. Furthermore, the previous approaches in TPP based interaction forecasting use negative sampling to approximate the loss associated with survival function, which is intractable to calculate due to the huge number of possible event types in the TPP.

This can introduce biases in training, especially in these complex interactions. To address these challenges, we propose the model *Relational Recursive Hyperedge Temporal Point Process* (RRHyperTPP), and the following are the contributions of our work, (i) A contrastive learning strategy for higher-order interaction for hyperedge events in networks. This provides a more principled way of training our model without maximum likelihood estimation, thereby avoiding the computationally expensive survival function calculation. Our model performs better than the previous models that use negative sampling; (ii) New deep learning architecture for learning node representation from higher-order interaction. This involves two stages: interaction update and temporal drift. Interaction update is used to revise the node representation when an event involving it occurs by using the features of the type of interaction. Temporal drift is used to model the evolution of node representation during the interevent period using time projection based on JODIE [21] or Neural ODE [6] or time embeddings based on Fourier time features [9]; (iii) A new method for hyperedge link prediction for multi-relational recursive hypergraphs; (iv) Curated eight datasets for temporal multi-relational recursive hypergraphs; (v) Extensive experiments are done to show the advantage of our model over existing state-of-the-art models.

2 RELATED WORKS

The current works on interaction forecasting on networks are of two kinds, the ones that are trained using TPP loss and the ones that are using link prediction. The models in the first category parameterize the probability density function of a Neural Temporal Point Process with edges as the mark associated with events [28]. These involve models DeepCoevolve [10], DyReP [30], DSPP [5], and GNPP [33] that uses neural networks to parameterize the conditional intensity function of a TPP based on the nodes involved in the edges. These works mostly focus on interaction forecasting on bipartite and homogeneous networks. More recently, GHNN [17] defined TPPs on Temporal Knowledge Graphs where entities of different kinds and interactions are associated with relation type. However, all these models are developed for pair-wise interaction forecasting and cannot accurately model the higher-order interactions. Recent work [15] modeled higher-order interactions as hyperedge event formation in a network. Although this model can capture interactions between any number of nodes, it does not consider the internal groupings of nodes or their relationships with other nodes, such as in email exchanges or co-authorship networks.

The works in the second category use graph representation learning to learn continuous-time representations for the nodes that are then used to predict links using a binary scoring function. This involves models like JODIE [21], TGAT [9], and TGN [27]. These models can only predict the presence of an interaction at a given time and cannot answer temporal queries like when two nodes will interact or the time of the next interaction.

3 PRELIMINARIES AND PROBLEM STATEMENT

Hypergraph. A Hypergraph is denoted by the tuple $\mathcal{G} = (\mathcal{V}, \mathcal{H})$, where $\mathcal{V} = \{v_1, v_2, \dots, v_{|\mathcal{V}|}\}$ is the set of nodes, \mathcal{H} is the set of hyperedges with $\mathcal{H} \subset C(\mathcal{V})$ and $C(\mathcal{V})$ is the powerset of \mathcal{V} .

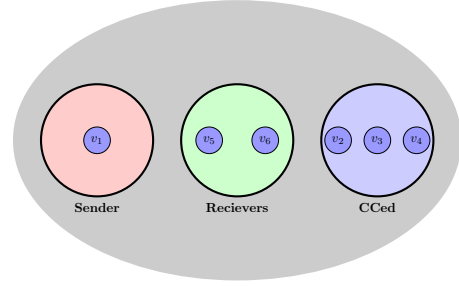


Figure 1: Email exchange between a group of people is represented as a Relational Recursive Hyperedges depth. Here, the sender involves a single person and multiple persons are in CCed and Receiver groups.

Recursive Hypergraph. A Recursive Hypergraph $\mathcal{G} = (\mathcal{V}, \mathcal{H})$ is a generalization of Hypergraph, where hyperedges can contain nodes and other hyperedges. Let, $\mathcal{H}^l = C(\cup_{i=0}^{l-1} \mathcal{H}^i)$ if $l \geq 1$, where $\mathcal{H}^0 = C(\mathcal{V})$. A recursive hypergraph is of depth l if $\mathcal{H} \subset \mathcal{H}^l$.

This work focuses on recursive hypergraphs of depth one and two. The following is the experimental setting followed in this paper.

Temporal Multi-relational Recursive Hypergraphs. A Temporal Multi-relational Recursive hypergraph is denoted by tuple $\mathcal{G}(t) = (\mathcal{V}, \mathcal{H}, \mathcal{R}, \mathcal{E}(t))$, where $\mathcal{E}(t) = \{(e_1, t_1), \dots, (e_n, t_n)\}$ is the ordered set of historical events till time t with $e_n \in \mathcal{H}$ and n is number events occurred and \mathcal{R} is the set of relation. Here, each hyperedge $h \in \mathcal{H}$ is formed of a set of recursive hyperedges, $h = h^l = \{(h_1^{l-1}, r_1^{l-1}), \dots, (h_{k^{l-1}}^{l-1}, r_{k^{l-1}}^{l-1})\}$ of depth l . Here, $r_i^{l-1} \in \mathcal{R}$ is the relation of hyperedge h_i^{l-1} with respect to hyperedge h^l , and $h_i^{l-1} \in \mathcal{H}^{l-1}$. Here, k^{l-1} is the number of relational groups, or depth zero hyperedges in hyperedge h , and $\mathcal{E}(t_a, t_b)$ is the ordered set of events observed during the interval $[t_a, t_b]$.

Using the above definition, we can represent a *Directed temporal hypergraph* by using relations indicating the source and destination groups, here $|\mathcal{R}| = 2$. Furthermore, including the node type attribute, we can extend this definition to a *Bipartite Temporal Hypergraph* where the nodes set is a union of two types, $\mathcal{V} = \mathcal{U}^r \cup \mathcal{U}^l$. Here, \mathcal{U}^r and \mathcal{U}^l are the two sets of nodes, and all interactions are between them. To use this framework for *Temporal Knowledge Graph* (TKGs) where interactions are represented as a triplet of the subject entity v^s , object entity v^o , and relation r between them, $h = (v^s, r, v^o)$. Here, $v^s, v^o \in \mathcal{V}$. This can be framed as a Multi-relational Recursive Hypergraph with $h = \{(h_0^0, r_1^0), (h_1^0, r_2^0)\}$. Here, $r_1^0 = r, r_2^0 = r^{-1}$ is the inverse relation, $h_0^0 = \{v^s\}$, and $h_1^0 = \{v^o\}$.

Problem. Given $\mathcal{E}(t) = \{(e_1, t_1), \dots, (e_n, t_n)\}$ historical interactions until time $t > t_n$, we aim to forecast the next interaction (t_{n+1}, e_{n+1}) where $t_{n+1} > t > t_n$. Here, we want to estimate the time t_{n+1} and the type of interaction e_{n+1} .

This work mainly focuses on higher-order interactions in communications networks and real-world events stored in source and target entities. The higher-order interaction in communications networks is represented using a recursive hyperedge graph of

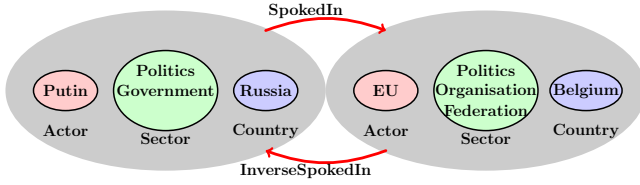


Figure 2: Real world events represented as Relational Recursive Hyperedges. Here, there are source and target hyperedges with three relations inside them and a relation type indicating the nature of the interaction.

depth one $h = \{(h_i^0, r_i^0)\}_{i=0}^{k_0}$. Here, relations are used to represent $\{r_i^0\}_{i=0}^3$ the sender, recipients, and carbon-copied recipients' addresses in case of email exchange and $\{r_i^0\}_{i=0}^4$ represents the sender, receiver, retweeter, and retweeted nodes in Twitter network. Figure 1 shows an email exchange as a higher-order interaction of depth one. The e higher-order interaction in real-world events is represented using depth two hypergraphs $h = \{(h_0^1, r_0^1), (h_1^1, r_1^1)\}$ and $h_{0/1}^1 = \{(h_i^0, r_i^0)\}_{i=0}^3$. Here, h_0^1, h_1^1 are the two entities involved in the interactions, r_0^1 and r_1^1 are the inverse relation pair indicating the type of interactions, $\{r_i^0\}_{i=0}^3$ is relation indicating the actor, sector, country of the entity. Figure 2 shows an example of this type of higher-order interaction.

4 RRHYPERTPP MODEL

The probability of the occurrence of hyperedge event h at time t is defined as follows,

$$P_h(t) = \lambda_h(t) S_h(t_h^p, t). \quad (1)$$

Here, $\lambda_h(t)$ is the conditional intensity function of the temporal point process, $S_h(t_h^p, t)$ is the survival function that denotes the probability that the event does not occur during the interval $[t_h^p, t]$,

$$S_h(t_h^p, t) = \exp\left(-\int_{t_h^p}^t \lambda_h(\tau) d\tau\right). \quad (2)$$

In this, $t_h^p < t$ is the time of the last occurrence of hyperedge h before time t , and it is initialized to zero for all the hyperedges at the beginning. The complete likelihood for observing $\mathcal{E}(T) = \{(e_1, t_2), \dots, (e_N, t_N)\}$ in the interval $[0, T]$ can be written as,

$$P(\mathcal{E}(T)) = \prod_{n=1}^N P_{e_n}(t_n) \prod_{h \in \mathcal{H}} S_h(t_h^p, T). \quad (3)$$

Here, t_h^p is the last occurrence of hyperedge h with $t^p = 0$ for $h \in \mathcal{H}$ that is not observed in the training data.

$$\begin{aligned} P(\mathcal{E}(T)) &= \prod_{n=1}^N \lambda_{e_n}(t_n) S_{e_n}(t_{e_n}^p, t_n) \prod_{h \in \mathcal{H}} S_h(t_h^p, T), \\ P(\mathcal{E}(T)) &= \prod_{n=1}^N \lambda_{e_n}(t_n) \prod_{h \in \mathcal{H}} S_h(0, T). \end{aligned} \quad (4)$$

For learning the parameters of conditional intensity $\lambda_h(t)$, we calculate the loss by taking a negative log-likelihood as shown below,

$$\mathcal{NLL} = -\sum_{n=1}^N \log \lambda_{e_n}(t_n) + \sum_{h \in \mathcal{H}} \int_0^T \lambda_h(t) dt. \quad (5)$$

However, direct minimization of the above loss function is computationally expensive due to the summation over all possible hyperedges in the survival function, which have an exponential number of possibilities, and also due to the integral over the entire duration of observation $\int_0^T (\cdot)$. So, to avoid these difficulties in computing the likelihood, we use the noise contrastive estimation technique of learning multivariate temporal point process [24] as explained in Section 4.1.

Furthermore, defining separate conditional intensity functions for each hyperedge will lead to difficulty in learning, as the number of parameters will increase linearly to the number of hyperedges, which is exponential on the order of the number of nodes, as explained earlier. It leads to overfitting while training and poor generalization in the test set. Hence, we define the conditional function as a positive function of dynamic embeddings nodes involved in it, $\lambda_h(t) = f(h; \mathbf{V}(t), \mathbf{R})$. Here, $\mathbf{V}(t)$ is the dynamic node embedding of nodes at time t , and \mathbf{R} is the relation embeddings. In this model, the number of parameters will be linear to the number of nodes, as hyperedges that share nodes will share the respective parameters.

4.1 Learning and Inference

An alternate approach to MLE for learning parameters is to use noise contrastive estimation (NCE). To achieve this, we discretize the training period $[0, T]$ into intervals of size Δt and simulate N_q noise streams $\{\mathcal{E}^i(t, t + \Delta t)\}_{i=1}^{N_q}$ from the noise distribution $Q(\cdot|\mathcal{E}(t))$ in addition to observed data $\mathcal{E}^0(t, t + \Delta t) = \mathcal{E}(t, t + \Delta t)$. In the following section, we will also use the zeroth index to denote the observed events for ease of depiction. Then the model parameters are trained to discriminate true and noise events from the candidate set $\{\mathcal{E}^i(t, t + \Delta t)\}_{i=0}^{N_q}$. This can be written as follows,

$$\begin{aligned} &\log\left(P^*\left(\mathcal{E}^0(t, t + \Delta t)\right) \prod_{i=1}^{N_q} Q^*(\mathcal{E}^i(t, t + \Delta t))\right) - \\ &\log\left(\sum_{i=0}^{N_q} P^*(\mathcal{E}^i(t, t + \Delta t)) \prod_{j \neq i, j=1}^{N_q} Q^*(\mathcal{E}^j(t, t + \Delta t))\right). \end{aligned}$$

Here, $P^*(\cdot) = P(\cdot|\mathcal{E}(t))$ and $Q^*(\cdot) = Q(\cdot|\mathcal{E}(t))$. However, we still need to calculate the integral $\sum_{h \in \mathcal{H}} \int_t^{t+\Delta t}$ in the probability density function, which is still computationally expensive. The solution is to shrink the interval to an infinitesimal width of dt when $\lim dt \rightarrow 0$. Then we can rewrite the above equation as,

$$\begin{aligned} &\log\left(P^*\left(\mathcal{E}^0(t, t + dt)\right) \prod_{i=1}^{N_q} Q^*(\mathcal{E}^i(t, t + dt))\right) - \\ &\log\left(\sum_{i=0}^{N_q} P^*(\mathcal{E}^i(t, t + dt)) \prod_{j \neq i, j=1}^{N_q} Q^*(\mathcal{E}^j(t, t + dt))\right). \end{aligned}$$

Here, in the interval $[t, t + dt]$, an event will be observed $\mathcal{E}^0(t, t + dt) = \{(h, t)\}$ or a null event will be observed $\mathcal{E}^0(t, t + dt) = \{(\emptyset, t)\}$

with respect to the distribution $P^*(\mathcal{E}^0(t, t + dt))$. So, the probability distribution should satisfy the following inequality at the interval $[t, t + dt]$,

$$\begin{aligned} & \sum_{h \in \mathcal{H}} P^*(\mathcal{E}^0(t, t + dt) = (h_i, t)) + \\ & P^*(\mathcal{E}^0(t, t + dt) = (\emptyset, t)) = 1, \\ & \sum_{h \in \mathcal{H}} \lambda_h(t) dt + P^*(\mathcal{E}^0(t, t + dt) = (\emptyset, t)) = 1. \end{aligned} \quad (6)$$

Here, $P^*(\mathcal{E}^0(t, t + dt) = \{(h, t)\}) = \lambda_h dt$ from the temporal point process conditional intensity function definition, and

$$P^*(\mathcal{E}^0(t, t + dt) = (\emptyset, 1)) = 1, \text{ when } dt \rightarrow 0.$$

Similarly, we can define $Q^*(\mathcal{E}^i(t, t + dt))$ using its definition of conditional intensity function. As a result of this, our objective function when there are no events in the observed stream $\mathcal{E}^0(t, t + dt) = (\emptyset, t)$ and in the N^q noise streams $\{\mathcal{E}^i(t, t + dt) = \{(\emptyset, t)\}\}_{i=1}^{N^q}$ becomes $\log \frac{1}{N^q + 1}$. However, when event h occurs in the true data stream or the noise data stream. The loss could be written as follows,

$$\begin{aligned} & \log \frac{\lambda_h(t)}{\lambda_h(t) + \lambda_h^q(t) N^q} \text{ if } \mathcal{E}(t, t + dt) = \{(h, t)\} \text{ else,} \\ & \text{for } i = 1 \text{ to } N^q, \\ & \log \frac{\lambda_h^q(t)}{\lambda_h(t) + \lambda_h^q(t) N^q} \text{ if } \exists \mathcal{E}^i(t, t + dt) = \{(h, t)\}. \end{aligned} \quad (7)$$

The complete loss function for the noise contrastive estimation can be written as follows,

$$\begin{aligned} \mathcal{L}_{NCE} = & -\mathbf{E}_{\mathcal{E}(T) \sim P(\cdot), \{\mathcal{E}^i(T)\}_{i=1}^{N^q} \sim Q(\cdot)} \left[\sum_{\mathcal{E}(t, t+dt) = \{(h, t)\}} \right. \\ & \left. \log \frac{\lambda_h(t)}{\lambda_h(t)} + \sum_{i=1}^{N^q} \sum_{\mathcal{E}^i(t, t+dt) = \{(h, t)\}} \log \frac{\lambda_h^q(t)}{\lambda_h(t)} \right]. \end{aligned} \quad (8)$$

Here, $\lambda_h(t) = \lambda_h(t) + \lambda_h^q(t) N^q$. In the above equation, we contrast the samples from the true distribution, the observed data, to the N^q independently sampled noise stream conditioned on the observed true historical data. A more detailed explanation of this contrastive loss function and the optimality of this technique can be found in the work of Mei et al. [24].

Additionally, to direct the gradients towards better model parameters, we add a classification-based noise contrastive loss at the time of the event as follows,

$$\mathcal{L}_{NCE}^s = \sum_{(e_n, t_n) \in \mathcal{E}(T)} \log \frac{\lambda_{e_n}(t)}{\lambda_{e_n}(t) + \sum_{h \in \mathcal{H}_{e_n}^{neg}} \lambda_h(t)}. \quad (9)$$

Here, $\mathcal{H}_{e_n}^{neg}$ are the negative samples generated by negative sampling for the hyperedge e_n . Then the combined loss can be written as follows,

$$\text{Loss} = \mathcal{L}_{NCE} + \alpha \mathcal{L}_{NCE}^s. \quad (10)$$

Here, α is a hyperparameter.

Algorithm 1 Training procedure of RRHyperTPP

Input: $\mathcal{G}(T)$.

while not convergence **do**

$\mathcal{H}^{neg} \sim \text{CorruptionModel}(\mathcal{H})$.

$\mathcal{H}^c = \mathcal{H} \cup \mathcal{H}^{neg}$.

Set $t = t_0 = 0$, $n = 1$, $\mathcal{L}_{NCE} = 0$.

for $n \leq N$ **do**

while $t < t_n$ **do**

Sample $\lambda^q(t) \sim \frac{1}{N^q w} \sum_{i=1}^{N^q} \mathcal{K}(\lambda^q - \frac{1}{t_i - t_{i-1}}; w)$.

Sample $\Delta t \sim \text{exponential}(N^q \lambda^q(t))$.

Sample $h \sim \text{Uniform}(\mathcal{H}^c)$.

Next event time $t = t + \Delta t$.

Loss = Loss - $\log \frac{\lambda_h^q(t)}{\lambda_h(t)}$

end while

$\mathcal{H}_{e_n}^{neg} \sim \text{CorruptionModel}(e_n)$

Loss = Loss - $\log \frac{\lambda_{e_n}(t)}{\lambda_{e_n}(t)}$

Loss = Loss - $\alpha \log \frac{\lambda_{e_n}(t)}{\lambda_{e_n}(t) + \sum_{h \in \mathcal{H}_{e_n}^{neg}} \lambda_h(t)}$

$n = n + 1$.

If $n \bmod B = 0$, Update the model parameters by AdamW Optimizer and set Loss = 0.

end for

end while

4.2 Noise Distribution

Here, we propose a method for simulating noise sequences by modeling the conditional distribution $Q^*(\mathcal{E}^i(t, t + dt) = \{(h, t)\})$. The thinning algorithm is a popular method for simulating a non-homogeneous Poisson process [7]. This way of sampling is computationally expensive if the acceptance probability is low. Moreover, modeling each hyperedge as a non-homogeneous Poisson process does not avoid the computational complexity of having many event types.

To overcome these limitations and accelerate training, we model the rate of events λ^q using a stochastic process independent of the event type and time. The probability density function of this process is learned from the observed event times in the training data $\mathcal{E}(T)$ using kernel density estimation [29], $\lambda^q \sim \frac{1}{N^q w} \sum_{i=1}^{N^q} \mathcal{K}(\lambda^q - \frac{1}{t_i - t_{i-1}}; w)$. Here, \mathcal{K} is the kernel, and w is the bandwidth of the kernel. We use the Gaussian kernel, and bandwidth is learned from the dataset. This will allow for a closed-form sampling of noise event times. Then we generate the type of event by uniformly sampling from a set of candidate hyperedges \mathcal{H}^c . Then $\lambda_h^q = \frac{1}{|\mathcal{H}^c|} \lambda^q$ and $Q(\mathcal{E}^i(t, t + dt) = \{(h, t)\}) = \frac{1}{|\mathcal{H}^c|} \lambda^q \exp(-\lambda^q(t - t_n))$.

The set of candidate hyperedges, denoted as \mathcal{H}^c , is formed by combining the true hyperedges observed in the training data with the negative hyperedges generated through the corruption of observed hyperedges. For depth one hyperedge datasets, we expand the hyperedge as a tuple of node and relation pairs in ascending order. Then we learn the categorical distribution of each position condition on all the previous relations, along with an end state. Then for each positive hyperedge, we first sample the relations till the end state is observed. Subsequently, we randomly populate each

position in the negative hyperedge with nodes. This is done by filling each position with nodes from the true hyperedge or randomly sampled nodes without repeating if they have the same relation value. This is done in such a way that at most half of the nodes of negative hyperedges are nodes from true hyperedge, and the rest is filled in randomly, thereby ensuring diversity in negative samples. For depth two hyperedge datasets, we randomly corrupt any one of the depth one hyperedge within them by the above procedure to generate negative hyperedges. Here, for each observed hyperedge $h \in \mathcal{H}$, we generate $N^e = |\mathcal{H}_h^{neg}|$ negative hyperedges.

For generating N^q noise streams, we multiply the noise distribution intensity function by N^q , $\lambda^q(t)N^q$, and simulated samples. This scaling will not affect NCE loss Equation 8, as all the noise streams have the same intensity values.

Algorithm 1 summarizes the entire training procedure of the model. The CorruptionModel(.) is the negative hyperedge generation function, and Uniform(\mathcal{H}^c) uniformly samples a hyperedge from the candidate hyperedges, \mathcal{H}^c . In the following section, we explain the dynamic node representation learning used to parameterize the conditional intensity function of the model. In our implementation, we use the same negative samples to generate the noise stream and in the supervised noise contrastive loss in Equation 9, $\mathcal{H}^n = \cup_{h \in \mathcal{H}} \mathcal{H}_h^{neg}$.

5 DYNAMIC NODE REPRESENTATION

The dynamic node representation of the nodes $\mathbf{V} \in \mathbb{R}^{|\mathcal{V}| \times d}$ in the networks are learned using a continuous time recurrent-neural network model using two stages, i) **Node Update** and ii) **Drift**, for node evolution.

5.1 Node Update

This stage is used to update the representation of a node v when it is involved in an interaction $h = \{(h_1^{l-1}, r_1^{l-1}), \dots, (h_{k^{l-1}}^{l-1}, r_{k^{l-1}}^{l-1})\}$ at time t . The update equation uses a recurrent neural network-based architecture that updates the node’s previously stored embedding based on the features of interaction calculated as follows,

$$\begin{aligned} i_v^h &= \text{MLP}\left(\left[\mathbf{d}_v^h; \mathbf{v}(t^-); \Psi(t - t_v^p)\right]\right) \\ \mathbf{v}(t^+) &= \text{RNN}(\mathbf{v}(t_v^p), i_v^h). \end{aligned} \quad (11)$$

Here, $v \in h^0$, $(h^0, r^0) \in \dots \in h$ and MLP is a two-layer multi-layer perceptron as shown below,

$$i_v^h = \mathbf{W}_1^i \tanh\left(\mathbf{W}_0^i \left[\mathbf{d}_v^h; \mathbf{v}(t^-); \Psi(t - t_v^p)\right]\right).$$

Here, $\mathbf{W}_0^i \in \mathbb{R}^{d^*(l+3) \times d^*(l+3)/2}$, $\mathbf{W}_1^i \in \mathbb{R}^{d^*(l+3)/2 \times d}$ are learnable parameters and $\mathbf{d}_v^h \in \mathbb{R}^d$ is the dynamic embedding calculated as a function of embeddings of other nodes involved in the interaction, $\mathbf{d}_v^h = f_{dyn}(h; \mathbf{V}(t), \mathbf{R})$. The architecture of $f_{dyn}(\cdot)$ is shared with hyperedge link prediction as explained in Section 6. The second term $\Psi(t - t_v^p) \in \mathbb{R}^d$ is the Fourier features for a time calculated based on the duration since an event was observed on v , $(t - t_v^p)$. Here, t_v^p is the recent time node v is involved in an interaction, and Fourier time features [9] are defined as $\Psi(t) = [\cos(\omega_1 t + \phi_1), \dots, \cos(\omega_d t + \phi_d)]$, where $\{\omega_i\}_{i=1}^d$, and $\{\phi_i\}_{i=1}^d$ are learnable parameters. When v is involved in multiple positions in hyperedge h , an average of i_v^h is taken to update the node embedding.

5.2 Drift

This stage is used for modeling the evolution of the nodes during the inter-event period. This helps to avoid the staleness of node embeddings due to not observing any event for a long duration [19].

Time Projection. In this technique, we project the node embeddings from the node update stage based on the elapsed time since the last update as follows,

$$\mathbf{v}(t) = (1 + \mathbf{W}_t(t - t_v^p)) \circ \mathbf{v}(t_v^p). \quad (12)$$

Here, $\mathbf{W}_t \in \mathbb{R}^{d \times d}$ is a learnable parameter, and \circ denotes the Hadamard product. This version of the embedding projection was introduced in the work JODIE [21].

Time Embeddings. Here, we use Fourier time features to model the evolution of the nodes during the interevent time as follows,

$$\mathbf{v}(t) = \tanh(\mathbf{W}_s \mathbf{v}(t_v^p) + \mathbf{W}_t \Psi(t - t_v^p)). \quad (13)$$

Here, $\mathbf{W}_s, \mathbf{W}_t \in \mathbb{R}^{d \times d}$ are learnable parameters. This form of drift stage is followed in previous work [15].

Neural ODE. The node embedding evolution is modeled using a neural Ordinary Differential Equation (ODE) as follows,

$$\mathbf{v}(t) = \mathbf{v}(t_v^p) + \int_{t_v^p}^t f_{\nabla \mathbf{v}}(\mathbf{v}(t), t - t_v^p) dt. \quad (14)$$

Here, $f_{\nabla \mathbf{v}}$ is the gradient of the node embedding $\mathbf{v}(t)$. We implement it using a multi-layer neural network that takes current node embedding and time elapsed since the last update as inputs to the network as shown below,

$$f_{\nabla \mathbf{v}}(\mathbf{v}(t), t - t_v^p) = \mathbf{W}_1^t \tanh\left(\mathbf{W}_0^t \left[\mathbf{v}(t); \mathbf{W}_t(t - t_v^p)\right]\right).$$

Here, $\mathbf{W}_t \in \mathbb{R}^{1 \times d}$, $\mathbf{W}_0^t \in \mathbb{R}^{2d \times d}$, $\mathbf{W}_1^t \in \mathbb{R}^{d \times d}$ are learnable parameters. Neural ordinary differential equations are infinite-depth deep learning models that are suited for modeling continuous dynamical systems. For training the models, we use the adjoint sensitivity method for reducing memory cost during back-propagation [6].

6 HYPEREDGE LINK PREDICTION

Given the node embeddings and relation embeddings of a hyperedge, we use the query-key-value attention mechanism used in transformer models [31] for hyperedge link prediction. For this, we first expand hyperedges at depth 0 as a tuple of node and relation pair and create an expanded depth one hyperedge $\bar{h}^0 = \{(v, r^0)\}_{v \in h^0, (h^0, r^0) \in h^1}$. Here, the relation is repeated for each node in the hyperedges. Then we create embeddings for query, key, and value, $\{\mathbf{v}_i^q(t) = \mathbf{v}_i^v(t) = [\mathbf{v}_i(t); \mathbf{r}_i^0]\}_{\forall (v_i, r_i^0) \in \bar{h}^0}$, then we calculate the dynamic hyperedge embedding (here, dynamic is used to indicate the hyperedge dependent embeddings \mathbf{d}_*^*) for each node as follows,

$$\mathbf{d}_v^{\bar{h}^0} = \text{MHAtt}(\{\mathbf{v}^q(t)\}, \{\mathbf{v}_j^k(t)\}_{j=1}^{\bar{k}^0}, \{\mathbf{v}_j^v(t)\}_{j=1}^{\bar{k}^0}). \quad (15)$$

Here, MHAtt(\cdot) is the MultiHeadAttention architecture proposed by Vaswani et al. [31]. Based on these, we create the depth one hyperedge embeddings by averaging out all the above node embeddings $\mathbf{h}_i^1 = \sum_{v \in \bar{h}^0} \frac{\mathbf{d}_v^{\bar{h}^0}}{|\bar{h}^0|}$. Then for the hyperedge at depths $2 \leq \ell \leq l$,

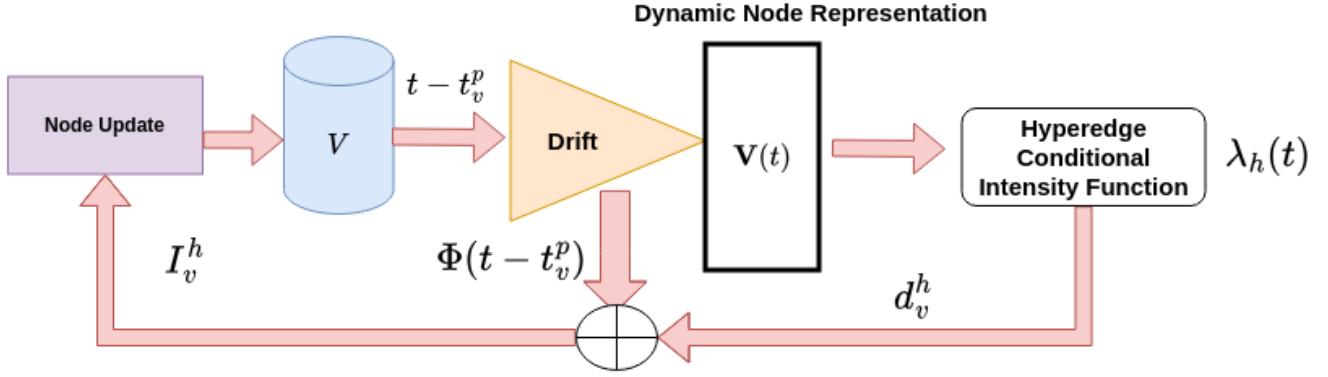


Figure 3: Deep Neural Network Architecture of RRHyperTPP: We calculate the dynamic node representation $V(t)$ by using Node Update (Section 5.1) and Drift (Section 5.2) stages. The node Update stage is used to update the node embeddings after an interaction involving that node occurs, and the Drift stage is used to model the evolution of node embedding during the interevent period. The dynamic node representation is used by the hyperedge link prediction-based decoder to infer the conditional intensity function $\lambda_h(t)$.

we apply the following self-attention layer with query, key, and value as $\{\mathbf{v}_i^q(t) = \mathbf{v}_i^k(t) = [\mathbf{h}_i^{l-1}(t); \mathbf{r}_i^{l-1}]\} \forall (\mathbf{h}_i^{l-1}, \mathbf{r}_i^{l-1}) \in h^l$,

$$\mathbf{d}_{h_i^{l-1}}^{h^l} = \text{MHAtt}(\{\mathbf{v}_i^q(t)\}, \{\mathbf{v}_j^k(t)\}_{j=1}^{k^{l-1}}, \{\mathbf{v}_j^v(t)\}_{j=1}^{k^{l-1}}),$$

$$\mathbf{h}^l = \sum_{(h_i^{l-1}, \mathbf{r}_i^{l-1}) \in h^l} \frac{\mathbf{d}_{h_i^{l-1}}^{h^l}}{|h^l|}. \quad (16)$$

Then conditional density is parameterized by the difference between the hyperedge embedding and dynamic hyperedge embedding of the $l-1$ th layer as follows,

$$o_i^h = \mathbf{W}_o (\mathbf{h}_i^{l-1} - \mathbf{d}_{h_i^{l-1}}^{h^l})^2 + b_o$$

$$\lambda_h(t) = \text{Softplus} \left(\sum_{(h_i^{l-1}, \mathbf{r}_i^{l-1}) \in h} o_i^h \right). \quad (17)$$

The dynamic hyperedge embedding used in the interaction update is defined as follows,

$$\mathbf{d}_v^h = [\mathbf{d}_v^{h^0}; \mathbf{d}_{h^0}^{h^1}; \dots; \mathbf{d}_{h^{l-1}}^{h^l}; \mathbf{h}^l],$$

here $v \in h^0, h^0 \in h^1, \dots, h^{l-1} \in h$.

7 EXPERIMENTAL SETTINGS AND RESULTS

7.1 Datasets

Table 1 shows the vital statistics of the datasets used in this work. In this, Enron is an email exchange dataset, and all the others, except the last two, are based on Twitter exchange. These datasets contain depth one hyperedges and are created from the works of Chodrow and Mellor [8], Domenico and Altmann [11], Omodei et al. [25]. ICEWS-India and ICEWS-Nigeria contain depth two hyperedges created from events stored in Integrated Crisis Early Warning System data for countries India and Nigeria [2]. For pre-processing, we have filtered out the nodes based on frequency, and all the timestamps start from zero and are scaled down so that the

mean interevent time is around one. Here, $\Delta t(\text{mean})$, $\Delta t(\text{max})$, and $\Delta t(\text{min})$ are the mean, maximum, and minimum interevent time.

7.2 Baselines

We use TGN [27] to compare our model's performance against state-of-the-art pairwise interaction prediction models. Additionally, we use HGDHE [15] to get a comparison against state-of-the-art higher-order interaction forecasting model that uses hyperedges to forecast interactions. Further, we created the model RRHyperTPP-N to show the advantage of our training strategy over negative sampling explored in previous work [15]. Here, we use time embeddings for drift to make the model closer to the one proposed in their work. Additionally, to show the advantage of the recursive hyperedge link prediction in Section 6, we created baseline model HyperTPP to forecast hyperedges created from the nodes involved in the interactions, $h = \{v_i; v_i \in h^0, (h^0, r^0) \in \dots \in h\}$, and this model is trained using the same loss as RRHyperTPP.

7.3 Forecasting Tasks And Evaluation Metrics

We use two tasks, (i) Interaction Type Prediction and (ii) Interaction duration Prediction, to evaluate our models' performance. In the first task, we are trying to predict which type of hyperedge occurs at time t given the history. This can be estimated by finding the hyperedge that has the maximum probability $P(\mathcal{E}(t, t+dt) = (h, t) | \mathcal{E}(t))$, which is equal to finding the hyperedge with maximum conditional intensity function as per definition of TPP, $\hat{h} = \arg \max_h \lambda_h(t)$. For evaluation, we calculate the Area Under the Curve (AUC) metric [13] by using the CorruptionModel to create N^e false positive samples for each true positive sample and then calculate the area under the curve. Here, better performance is indicated by values close to one. For the second task, we are trying to predict the time at which interaction h occurs from the last interaction duration of nodes in the hyperedge t_h^p . This is estimated using the condition probability density as $\hat{t}_i = \int_{t_h^p}^{\infty} t P_h(t | \mathcal{E}(t_h^p)) dt$. Here, $P_h(t | \mathcal{E}(t_h^p))$ is defined as in Equation 1, and all the integration involved are

Table 1: Temporal Multi-Relational Recursive Hypergraphs datasets and their vital statistics.

Datasets	$ \mathcal{V} $	$ \mathcal{E}(T) $	$ \mathcal{R} $	T	$\Delta t(\text{mean})$	$\Delta t(\text{max})$	$\Delta t(\text{min})$
Enron	98	10,355	3	10,443.0	1.02	893.45	0.006
Twitter	2,714	52,383	4	54,028	1.54	25.64	0.625
Boston	2,400	20,070	4	20,069	1.03	37.13	0.044
Obama	1,721	22,690	4	22,689	1.02	1628.61	0.021
Pope	6,648	67,779	4	67,778	1.07	68.97	0.047
Cannes	672	9,078	4	9,077	1.00	58.02	0.007
ICEWS-India	1,066	86,609	201	364	1.00	1.0	1.0
ICEWS-Nigeria	894	6,95,433	181	715	1.00	2.94	0.98

Table 2: Performance on forecasting in interaction type and interaction duration prediction tasks on depth one hyperedges. Here, interaction type prediction is evaluated using AUC in %, and interaction duration prediction is evaluated using MAE. The proposed model RRHyperTPP beats baseline models in almost in settings. Here, -j, -f, and -o indicate the drift stage used.

Methods	Enron		Twitter		Boston		Obama		Pope		Cannes	
	AUC	MAE	AUC	MAE	AUC	MAE	AUC	MAE	AUC	MAE	AUC	MAE
TGN [27]	85.8 ± 2.9	NA	97.0 ± 0.5	NA	89.3 ± 1.5	NA	93.0 ± 1.0	NA	92.5 ± 1.2	NA	87.6 ± 2.4	NA
HGDHE [15]	87.6 ± 0.8	3.6 ± 0.1	88.0 ± 1.1	26.26 ± 0.5	75.3 ± 1.3	49.16 ± 5.2	82.0 ± 0.1	29.8 ± 0.8	79.1 ± 0.3	33.6 ± 1.2	79.1 ± 1.0	27.9 ± 2.0
RRHyperTPP-N	91.0 ± 0.9	3.5 ± 0.0	94.2 ± 0.6	21.9 ± 0.4	80.8 ± 0.2	39.9 ± 0.1	85.2 ± 0.4	27.6 ± 0.6	82.5 ± 0.5	31.9 ± 0.3	81.9 ± 1.0	25.4 ± 1.8
HyperTPP-j	91.6 ± 0.7	3.3 ± 0.7	97.2 ± 0.0	30.0 ± 0.6	85.4 ± 0.8	46.5 ± 0.7	90.7 ± 0.3	35.5 ± 1.1	85.2 ± 6.0	40.1 ± 1.2	90.7 ± 1.04	24.0 ± 2.7
HyperTPP-f	90.8 ± 1.0	3.7 ± 0.3	97.3 ± 0.1	33.4 ± 0.5	83.4 ± 0.2	49.6 ± 2.1	86.6 ± 0.2	37.4 ± 1.5	91.8 ± 0.8	37.6 ± 0.2	86.4 ± 0.5	28.2 ± 2.1
HyperTPP-o	91.6 ± 0.5	3.7 ± 0.3	96.8 ± 0.3	30.8 ± 0.6	84.6 ± 1.2	51.8 ± 2.9	89.2 ± 0.5	38.6 ± 1.5	88.9 ± 1.4	37.3 ± 2.1	89.1 ± 1.6	26.8 ± 2.4
RRHyperTPP-j	93.3 ± 0.7	3.3 ± 0.2	98.5 ± 0.1	30.6 ± 1.8	89.2 ± 0.1	45.7 ± 0.4	93.5 ± 0.5	32.5 ± 0.4	94.2 ± 0.4	36.2 ± 1.0	92.1 ± 0.4	25.6 ± 1.5
RRHyperTPP-f	93.4 ± 0.3	3.5 ± 0.2	98.4 ± 0.1	32.3 ± 0.5	89.2 ± 0.2	45.1 ± 0.4	92.9 ± 0.3	31.8 ± 0.3	93.9 ± 0.3	37.6 ± 0.2	89.3 ± 0.4	25.2 ± 0.9
RRHyperTPP-o	93.5 ± 0.2	3.7 ± 0.1	98.3 ± 0.1	30.1 ± 0.9	88.0 ± 1.7	46.3 ± 3.1	92.3 ± 1.0	35.6 ± 2.0	94.0 ± 0.7	35.4 ± 1.2	91.2 ± 0.7	28.6 ± 0.6

computed using Monte-Carlo integration. Then, for evaluation, we use Mean Absolute Error (MAE) metric, $MAE = \frac{1}{N} \sum_{i=1}^N |\hat{t}_i - t_i|$ for all the samples in the test.

7.4 Parameter Settings

In all our experiments, we fixed the embedding dimension at $d = 64$, hidden and input dimension for the RNN at 64, batch size $B = 128$, number of noise streams $N^q = 20$, number of corrupted hyperedges per true hyperedge is $N^e = 20$, and number heads of MHAtt to four. The training is done for 200 epochs, and the model parameters that gave the least validation score $\mathcal{L}_{NCE} + \alpha \mathcal{L}_{NCE}^s$ are used for testing. For all the training, we use the AdamW optimizer [23, 26] of PyTorch [20] with learning rate set to 0.0005. The first 50% of interactions is used for training, the next 25% for validation, and the rest for testing.

7.5 Results

Table 2 shows the performance of our models RRHyperTPP against baseline models. Here, the models that use time projection, ODEs, and time embeddings for **Drift** stage are denoted by -j, -o, and -f at the end, respectively. In this, models that use ODE for the drift stage perform slightly less than ones that use other techniques. This is due to numerical issues involved with Neural ODE training, which involves computing integral in the gradient backpropagation. However, theoretically, Neural ODEs should perform better than others as they have fewer assumptions when compared to Fourier

Table 3: Performance on forecasting in interaction type and interaction duration prediction tasks on depth two hyperedges.

Methods	ICEWS-India		ICEWS-Nigeria	
	AUC	MAE	AUC	MAE
RRHyperTPP-j	58.7 ± 0.7	0.99 ± 0.0	61.0 ± 0.3	0.98 ± 0.0
RRHyperTPP-f	58.9 ± 0.2	0.75 ± 0.2	60.5 ± 0.5	0.81 ± 0.1
RRHyperTPP-o	58.2 ± 1.4	0.99 ± 0.0	58.7 ± 0.3	0.97 ± 0.0

and time projection-based methods. We have also done experiments on depth two hyperedges, and the results are shown in Table 3. Here, we can also observe that no single model outperforms the rest in all the tasks. Further, there is an average increment of 3.6% in the AUC metric for RRHyperTPP models when compared to HyperTPP based models in interaction type prediction tasks. For the interaction duration prediction task, we observed a reduction of 4.6% MAE when compared to HyperTPP models. Hence, we can conclude that modeling the recursive group structure of interaction resulted in performance improvement. Hence, more exploration is needed to find a better noise generation strategy to achieve better performance simultaneously in both tasks.

Moreover, we compare our model against TGN, a state-of-the-art pairwise interaction forecasting model. For the task of interaction type prediction, we can observe an increment of 2.9%, 2.3%, and 2.2%

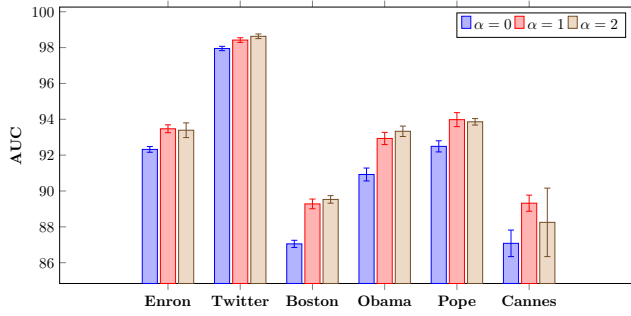


Figure 4: The performance gain obtained due to the addition of classification based noise contrastive loss mentioned Equation 10. Here, we can observe that models trained with supervised noise contrastive loss $\alpha > 0$ have more AUC scores for interaction type prediction than models that do not ($\alpha = 0$).

for models RRHyperTPP-j, RRHyperTPP-f, and RRHyperTPP-o, respectively. Hence, we can conclude that recursive hyperedge-based models perform better than pairwise link prediction models. Similarly, we compared our model RRHyperTPP-f against the HGDHE state-of-the-art hyperedge forecasting model, as both use time embeddings for the drift stage. Here, we can observe a gain of 13.6% in AUC for interaction type prediction. We can observe similar improvements for other types of drift when compared to HGDHE model.

To show the advantage of our training strategy over negative sampling-based loglikelihood approximation followed in the previous work by [15], we compare models RRHyperTPP-f against RRHyperTPP-N. Here, both models use the same architecture, but the former uses the noise-contrastive loss for training, and the latter uses negative sampling based on approximate negative loglikelihood. There is an average improvement of 8.2% in AUC for RRHyperTPP-f models compared to RRHyperTPP-N. However, there is an average increase of 15.3% in MAE for RRHyperTPP-f compared to RRHyperTPP-N. Hence, more exploration is needed to find a better noise generation strategy to achieve better performance simultaneously in both tasks. Further, RRHyperTPP-N has an improvement of 4.9% in AUC and 9.8% reduction in MAE over previous work HGDHE, which uses hyperedge to represent higher-order interaction. Hence, we can conclude that multi-relational recursive provides better representation for higher-order interactions than hyperedges.

Performance gain due to supervised NCE. Figure 4 illustrates the performance improvement in AUC of RRHyperTPP-f with different weights of the supervised noise contrastive loss in Equation 10 for the interaction type prediction task. Here, it can be observed that when $\alpha = 1$, there is a 1.7% increase in AUC compared to $\alpha = 0$. Therefore, we infer that the supervised noise contrastive loss enhances performance. Additionally, it can be noted that when α is increased to two, there are no significant improvements, and a performance decrement is observed for the Cannes dataset. Consequently, we can conclude that increasing α will not yield better performance. Furthermore, we observed no significant improvement for the interaction duration prediction task by changing α .

8 CONCLUSION

In this work, we have shown the significance of using the multi-relational recursive hyperedges for interaction modeling as it is a more natural approximation of real-world events. Here, we created a dynamic node representation and link predictor framework that can use this intricate relationship of interactions to forecast future events. In addition, we also created a noise contrastive learning framework that avoids the integration calculation in the survival function and can train when the number of types of events is of exponential order. To evaluate the model, we curated six datasets of depth one and two datasets of depth two hyperedges. We observed that our model RRHyperTPP is performing better previous state-of-the-art graph link prediction model TGN, and the negative sampling-based training strategy followed in previous work by Gracious and Dukkupati [15]. As a future direction, we plan to explore new domains of application of these models and new architecture that uses higher-order information to learn efficient node representations. In addition to this, we also plan on improving the noise generation strategy by using historical data, so the noise-generated samples will look more closely to actual data, thereby reducing the training iterations.

REFERENCES

- [1] Adrian Baddeley, Imre Bárány, and Rolf Schneider. 2007. *Stochastic Geometry*. Springer Berlin Heidelberg. 1–75 pages.
- [2] Elizabeth Boschee, Jennifer Lautenschlager, Sean O’Brien, Steve Shellman, James Starz, and Michael Ward. 2015. ICEWS Coded Event Data.
- [3] Michael M Bronstein, Joan Bruna, Taco Cohen, and Petar Veličković. 2021. Geometric deep learning: Grids, groups, graphs, geodesics, and gauges. *arXiv preprint arXiv:2104.13478* (2021). arXiv:2104.13478
- [4] Michael M Bronstein, Joan Bruna, Yann LeCun, Arthur Szlam, and Pierre Vandergheynst. 2017. Geometric deep learning: Going beyond euclidean data. *IEEE Signal Processing Magazine* 34, 4 (2017), 18–42.
- [5] Jiangxia Cao, Xixun Lin, Xin Cong, Shu Guo, Hengzhu Tang, Tingwen Liu, and Bin Wang. 2021. Deep structural point process for learning temporal interaction networks. In *Machine Learning and Knowledge Discovery in Databases. Research Track*. 305–320.
- [6] Ricky T. Q. Chen, Yulia Rubanova, Jesse Bettencourt, and David K Duvenaud. 2018. Neural Ordinary Differential Equations. In *Advances in Neural Information Processing Systems*, Vol. 31.
- [7] Yuanda Chen. 2016. Thinning algorithms for simulating point processes.
- [8] Philip Chodrow and Andrew Mellor. 2019. Annotated hypergraphs: Models and applications. *Applied Network Science* 5 (2019), 1–25.
- [9] da Xu, chuanwei ruan, evren korpeoglu, sushant kumar, and kannan achan. 2020. Inductive representation learning on temporal graphs. In *International Conference on Learning Representations*.
- [10] Hanjun Dai, Yichen Wang, Rakshit Trivedi, and Le Song. 2016. Deep coevolutionary network: Embedding user and item features for recommendation. arXiv:1609.03675
- [11] Manlio De Domenico and Eduardo G. Altmann. 2020. Unraveling the origin of social bursts in collective attention. *Scientific Reports* 10 (2020), 4629.
- [12] Bahare Fatemi, Perouz Taslakian, David Vazquez, and David Poole. 2020. Knowledge Hypergraphs: Prediction Beyond Binary Relations. In *Proceedings of the Twenty-Ninth International Joint Conference on Artificial Intelligence (IJCAI)*. 2191–2197.
- [13] Tom Fawcett. 2006. An introduction to ROC analysis. *Pattern Recognition Letters* 27, 8 (2006), 861–874.
- [14] Yifan Feng, Haoxuan You, Zizhao Zhang, Rongrong Ji, and Yue Gao. 2019. Hypergraph neural networks. In *Proceedings of the AAAI Conference on Artificial Intelligence*, Vol. 33. 3558–3565.
- [15] Tony Gracious and Ambedkar Dukkupati. 2023. Dynamic representation learning with temporal point processes for higher-order interaction forecasting. In *Proceedings of the AAAI Conference on Artificial Intelligence*, Vol. 37. 7748–7756.
- [16] Mustafa Hajij, Ghada Zamzmi, Theodore Papamarkou, Nina Miolane, Aldo Guzmán-Saenz, Karthikeyan Natesan Ramamurthy, Tolga Birdal, Tamal K Dey, Soham Mukherjee, Shreyas N Samaga, et al. 2023. Topological deep learning: Going beyond graph data. arXiv:2206.00606
- [17] Zhen Han, Yunpu Ma, Yuyi Wang, Stephan Günnemann, and Volker Tresp. 2020. Graph Hawkes Neural Network for Forecasting on Temporal Knowledge Graphs.

- In *Automated Knowledge Base Construction*.
- [18] Max Horn, Edward De Brouwer, Michael Moor, Yves Moreau, Bastian Rieck, and Karsten Borgwardt. 2022. Topological graph neural networks. In *International Conference on Learning Representations*.
 - [19] Seyed Mehran Kazemi, Rishab Goel, Kshitij Jain, Ivan Kobyzev, Akshay Sethi, Peter Forsyth, and Pascal Poupart. 2020. Representation learning for dynamic graphs: A survey. *The Journal of Machine Learning Research* 21, 1 (2020), 2648–2720.
 - [20] Diederik P Kingma and Jimmy Ba. 2015. Adam: A Method for stochastic optimization. In *International Conference on Learning Representations*.
 - [21] Srijan Kumar, Xikun Zhang, and Jure Leskovec. 2019. Predicting dynamic embedding trajectory in temporal interaction networks. In *Proceedings of the 25th ACM SIGKDD international conference on Knowledge discovery and data mining*.
 - [22] Dongjin Lee and Kijung Shin. 2023. I’m Me, We’re Us, and I’m Us: Tri-directional Contrastive Learning on Hypergraphs. In *Proceedings of the AAAI Conference on Artificial Intelligence*.
 - [23] Ilya Loshchilov and Frank Hutter. 2019. Decoupled Weight Decay Regularization. In *International Conference on Learning Representations*.
 - [24] Hongyuan Mei, Tom Wan, and Jason Eisner. 2020. Noise-contrastive estimation for multivariate point processes. *Advances in Neural Information Processing Systems* 33 (2020), 5204–5214.
 - [25] Elisa Omodei, Manlio De Domenico, and Alex Arenas. 2015. Characterizing interactions in online social networks during exceptional events. *Frontiers in Physics* 3 (2015), 59.
 - [26] Sashank J. Reddi, Satyen Kale, and Sanjiv Kumar. 2018. On the Convergence of Adam and Beyond. In *International Conference on Learning Representations*.
 - [27] Emanuele Rossi, Ben Chamberlain, Fabrizio Frasca, Davide Eynard, Federico Monti, and Michael Bronstein. 2020. Temporal graph networks for deep learning on dynamic graphs. arXiv:2006.10637
 - [28] Oleksandr Shchur, Ali Caner Türkmen, Tim Januschowski, and Stephan Günemann. 2021. Neural Temporal Point Processes: A Review. In *IJCAI 2021*.
 - [29] Bernard W Silverman. 1986. *Density estimation for statistics and data analysis*. Vol. 26. CRC press.
 - [30] Rakshit Trivedi, Mehrdad Farajtabar, Prasenjeet Biswal, and Hongyuan Zha. 2019. DyRep: Learning Representations over Dynamic Graphs. In *International Conference on Learning Representations*.
 - [31] Ashish Vaswani, Noam Shazeer, Niki Parmar, Jakob Uszkoreit, Llion Jones, Aidan N. Gomez, Łukasz Kaiser, and Illia Polosukhin. 2017. Attention is all you need. In *Advances in Neural Information Processing Systems*, Vol. 30.
 - [32] Jianfeng Wen, Jianxin Li, Yongyi Mao, Shini Chen, and Richong Zhang. 2016. On the representation and embedding of knowledge bases beyond binary relations. In *Proceedings of the Twenty-Fifth International Joint Conference on Artificial Intelligence*. 1300–1307.
 - [33] Wenwen Xia, Yuchen Li, and Shenghong Li. 2022. Graph neural point process for temporal interaction prediction. *IEEE Transactions on Knowledge and Data Engineering* 35 (2022), 4867–4879.

A NOTATIONS

Tables 4 and 5 shows the notations and their respective definitions used in this paper. We used bold lower-case letters to show vectors and bold upper-case letters to show matrices.

Received 20 February 2007; revised 12 March 2009; accepted 5 June 2009

Table 4: Notations-I

Notation	Definition
$\mathcal{G} = (\mathcal{V}, \mathcal{H})$	Hypergraph
\mathcal{V}	Set of nodes
\mathcal{H}	set of edges
$C(\cdot)$	Power set
\mathcal{H}^l	Hyperedges at depth l
l	Depth
$\mathcal{G}(t) = (\mathcal{V}, \mathcal{H}, \mathcal{R}, \mathcal{E}(t))$	A temporal multi-relation recursive hypergraph
\mathcal{R}	Set of relations
N	Total number of events
t	Time
h	Hyperedge
k	Expanded hyperedge size
k^l	Number of depth l hyperedges in h
h^0	Hyperedge at depth 0
$h = \{(h_1^{l-1}, r_1^{l-1}), \dots, (h_{k^{l-1}}^{l-1}, r_{k^{l-1}}^{l-1})\}$	Recursive hyperedge of depth l
r_i^{l-1}	Relation of hyperedge h_i^{l-1} with respect to hyperedge h^l
$\lambda(t)$	Conditional intensity function
k	Hyperedge size
\mathcal{R}	Relation set $\mathcal{R} = \{r_1, \dots, r_{ \mathcal{R} }\}$
r^{-1}	Inverse relation
$\mathcal{U}^r, \mathcal{U}^l$	Right nodes and left nodes
$\mathcal{E}(t)$	Historical interactions till time t
e_n	n th event type
n	Event index
v^s	Subject entity
v^o	Object entity
t_v^p	Previous event time for node v_i
t_h^p	Previous event time for hyperedge h
dt	Derivative of time t
d	Embedding size
v_i	i th node
$\lambda_h(t)$	Conditional intensity function of interaction h
t_h^p	Previous time of interaction for hyperedge h

Table 5: Notations-II

Notation	Definition
$P_h(t)$	Probability of hyperedge event h happening at time t
$P^*(\cdot)$	$P(\cdot \mathcal{E}(t))$ conditional event distribution of the observed sequence
$Q^*(\cdot)$	$Q(\cdot \mathcal{E}(t))$ conditional event distribution of the noise sequence
$S_h(t_h^p, t)$	Survival function of hyperedge during the interval $[t_h^p, t]$
$d\tau$	Infinitesimal time
T	Observation interval
\mathcal{NLL}	Negative log-likelihood
N	Number of events in the interval $[0, T]$
t_h^l	Last event time for hyperedge h
Δt	Interevent time
$Q(\cdot)$	Noise distribution
\mathcal{E}^i	Noise stream i
N^q	Number of noise streams
N^e	Number of negative samples per observed hyperedge
\emptyset	Null event
$\lambda_h(t)$	conditional intensity function of combined event stream
\mathcal{H}^c	Candidate hyperedges
$\mathcal{H}_{e_n}^{neg}$	Negative hyperedges created for hyperedge e_n
\mathcal{K}	Kernel for KDE
w	Bandwith
λ^q	Rate of events
\mathcal{L}_{NCE}	Noise contrastive loss
\mathcal{L}_{NCE}^s	Supervised noise contrastive loss
B	Batch size
v	Node
\mathbf{d}_v^h	Dynamic hyperedge embedding
f_{dyn}	Function for dynamic hyperedge embedding
$\Psi(\cdot)$	Fourier features
$\{\omega_i\}_{i=1}^d$, and $\{\phi_i\}_{i=1}^d$	Parameters of Fourier features
t_v^p	Previous interaction time for node
\mathbf{v}	Node embeddings
\mathbf{i}_v^h	Interaction features
\mathbb{R}	Real space
\mathbf{W}_t	Temporal drift parameter
$f_{\nabla \mathbf{v}}$	Gradient of node embedding
$\mathbf{v}_i^q(t), \mathbf{v}_i^k(t), \mathbf{v}_i^v(t)$	Query, Key, Value embeddings
\bar{h}^0	Expanded hyperedge at depth 0
\bar{k}^0	Size of expanded hyperedge at depth 0
$\mathbf{d}_{h_i^{l-1}}^h$	Dynamic node embedding at depth l for for hyperedge h_i^{l-1}
\mathbf{h}_i^h	Hyperedge embedding
o_i^h	Output score for hyperedge link predictor
MHAtt(\cdot)	Multi-head attention layer